IMAGE FUSION AND WAVELET ANALYSIS FOR 3-D RECONSTRUCTION USING 2-D IMAGES OBTAINED UNDER DIFFERENT ILLUMINATION CONDITIONS

T. Heger, M. Pandit, R. Meisner

University of Kaiserslautern
Department of Electrical and Computer Engineering
Institute of Control Systems and Signal Theory
67653 Kaiserslautern – Germany
Thomas.Heger@eit.uni-kl.de

ABSTRACT

Capturing 3-d information using several 2-d images of topological 3-d objects obtained by acquiring the images under varying illumination conditions is a technique which can be employed in manufacturing systems. The paper deals with the tasks of acquiring the images from objects with hybrid reflecting behaviour and algorithms for extracting the 3-d information and gives results obtained for a grinding tool inspection system.

1. INTRODUCTION

Methods for obtaining qualitative shape information of objects by processing images of 3-d objects and their shadows is a known technique in image processing. The paper deals with the quantitative determination of the characteristics of a 3-d surface with hybrid reflecting behaviour by processing 2-d images $\mathbf{U}_{\alpha_i,\beta_j} = u(k,l;\alpha_i,\beta_j)$ obtained by acquiring the images under varying angles of illumination α_i, β_j.

The method has been developed for application in a wear assessment system for grinding tools in which the wear of the surface of the grinding tool is assessed by determining the temporal change in the distribution of the sizes and the number of embedded particles and those of the cavities left behind by dislodged particles.
The tasks involved in the process are:

1. Construction of a system consisting of a camera and an illumination dome capable of illuminating the surface from a pre-defined controllable angle.
2. Acquiring the grey value images $\mathbf{U}_{\alpha_i,\beta_j}$ corresponding to the pixels at the positions (k,l) and the illumination angles α_i (azimuth) and β_j (elevation).
3. Generation of a height image $\mathbf{H} = h(k,l)$ by data fusion of the grey value images $\mathbf{U}_{\alpha_i,\beta_j}$ where $h(k,l)$ represents an estimate of the altitude of the surface at the location (k,l).

In the actual wear assessment system in addition following tasks have to be performed:

4. Generation of an image in which the embedded particles and the cavities are identified, segmented and labeled correspondingly.
5. A histogram of the heights of the embedded particles which is a measure of the roughness of the surface. The roughness is the ultimate performance information.

For the application it is possible and advantageous to combine the Steps 3 and 4 for identification and segmentation. Additionally, Step 3 has to be performed explicitly or implicitly for achieving the goal of Step 5.

In this article we present a method for identifying and localizing *topological 3-d objects* (T3DO), like grains and cavities on the surface of a grinding tool, using wavelet analysis of the 1-d signals obtained along line scans of the 2-d images corresponding to various illumination angles α_i and $\beta = 15°$. This is the basis of capturing topological 3-d information which is currently under investigation.

2. DESCRIPTION OF THE IMAGE ACQUISITION SYSTEM

The image acquisition system consists of a hemispherical dome with LEDs as light sources placed on the inner surface at 8 azimuth angles $\alpha_i = i \cdot 45°$, i = 0,1,... 7 and 4 elevation angles $\beta_j = j \cdot 15°$, j = 1,2,3,4. Thus 32 different illumination angles are possible.

The images are taken with a CCD color camera. The lens setup is chosen to image an area of 2mm×1.5mm (lens–to–surface distance is 51mm) and the resolution is 800×600 pixels.

Four uni–directional illuminated images $\mathbf{U}_{\alpha_i,\beta_j}$ are presented in Fig. 10. It is clear to see that each of these images contains different information about the same scene due to

0-7803-8554-3/04/$20.00 ©2004 IEEE.

the topography of the surface ([4]). To get all relevant information about the scene into one image, the maximum (Eq. (1)) of all $\mathbf{U}_{\alpha_i,\beta_j}$ is taken to form the new image

$$\mathbf{M}_{\beta_j} = m(k,l;\beta_j) = \max_{\alpha_i}(u(k,l;\alpha_i,\beta_j)) \quad \text{with} \quad \alpha_i = i \cdot 45°, \text{ i = 0,1,... 7} \tag{1}$$

This fusion of the eight images greatly enhances the information of the scene (see Fig. 11). This image $\mathbf{M}_{\beta_j}$ is then used in Sec. 3 for the identification of the T3DO.

3. IDENTIFYING 3-D OBJECTS USING WAVELETS

An inspection of images containing topological 3-d objects (T3DO) (Fig. 11), reveals that most of the T3DO are represented by a bright border and a dark center (Fig. 1, black circle) due to their reflecting and shadowing behaviour. Based on this observation, a wavelet based method was found to be the most robust for the identification of T3DO with respect to brightness fluctuations of the image M_{β_j}, the varying size of the T3DO and noise in the background.

For identification of the T3DO, the characteristic wave forms of their grey values in the image $\mathbf{M}_{\beta_j}$ (see Fig. 1) are examined (see Fig. 2). Due to the time (or space) and frequency localization behaviour of the continuous wavelet transfom (CWT) (Eq. (2)), it can be used to identify known wave forms in different scales and positions.

$$W_\psi s(\alpha,\tau) = \frac{1}{\sqrt{\alpha}} \int_{-\infty}^{+\infty} s(t)\psi\left(\frac{\tau - t}{\alpha}\right) dt \tag{2}$$

(Here $W_\psi s(\alpha,\tau)$ is the wavelet transform and $\psi(t)$ is the wavelet function.)
Therefore we represent the grey value curve in Fig. 2 by its wavelet coefficients using a wavelet similar to the wave form to be detected (e.g. inverted Mexican-Hat). The position of the large wavelet coefficients (τ in Eq. (2)) is extracted to localize the T3DO.

The identification algorithm can be divided into three main parts:

1. Performing the wavelet transform
2. Evaluating the wavelet coefficients
3. Recovering an approximate shape of the identified T3DO using common methods.

3.1. Performing the wavelet transform

For a convenient implementation of the CWT, some sort of a multi-scale analysis has been adopted, where a subspace projection like in MSA, has been used.

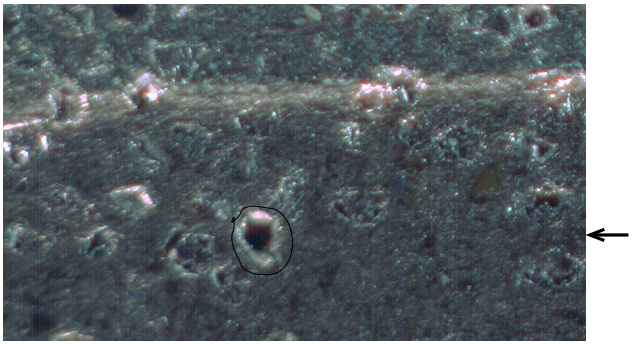

Fig. 1. Sample image $\mathbf{M}_{\beta_j}$ of a grinding tool surface with a marked T3DO (black circle)

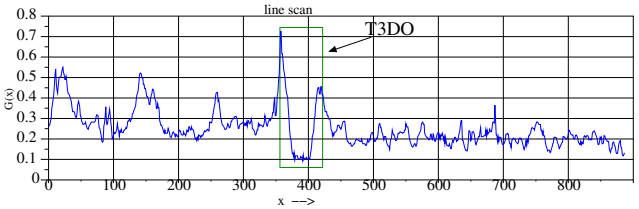

Fig. 2. Grey values of the marked line in image Fig. 1

The wavelet transform in Eq. (2) can be calculated by the convolution in Eq. (3).

$$W_\psi s(\alpha,\tau) = (s * \psi_\alpha)(\tau) \quad \text{with} \quad \psi_\alpha = \tfrac{1}{\sqrt{\alpha}}\psi\left(\tfrac{t}{\alpha}\right) \tag{3}$$

ψ_α can be approximated by its *orthogonal* projection onto a subspace using a scaling function φ with compact support. To speed up the calculation even more, instead of the analytic function φ, an approximation by its B-spline function approximation (Eq. (4)) is used.

$$\beta^n(x) = \sum_{j=0}^{n+1} \frac{(-1)^j}{n!}\binom{n+1}{j}(x-j)^n\mu(x-j) \quad \text{with} \quad \mu(t) = \begin{cases} 1 & \text{for } t \geq 0 \\ 0 & \text{for } t < 0 \end{cases} \tag{4}$$

When using B-splines for approximation, Eq. (5) is obtained.

$$q_j(k) = \langle \psi_{\alpha_j}, \beta_k^n \rangle \quad \text{with} \quad \beta_k^n = \beta^n(x-k) \tag{5}$$

To increase the spatial resolution of this approximation, an *oblique* instead of an orthogonal projection was chosen, to get even finer scales.

Please refer to [2], [3], and [5] for more details about this methods.

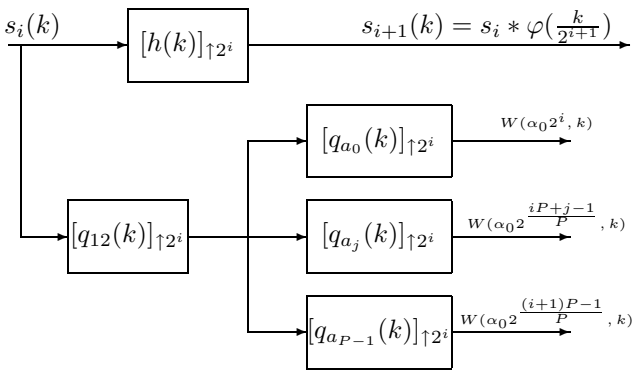

Fig. 3. Cascade of digital IIR and FIR filters to perform the wavelet transform

Finally, the CWT (MSA) can be computed by the following algorithm:

1. $s_{i+1}(k) = (s_i * [h]_{\uparrow 2^i})(k)$
2. $\tilde{s}_i(k) = (s_i * [q_{12}]_{\uparrow 2^i})(k)$
3. $\tilde{W}_\psi s(2^i \alpha_j, k) = (\tilde{s}_i * [q_{\alpha_j}]_{\uparrow 2^i})(k)$

where $[q_{12}]_{\uparrow 2^i}$ is an IIR filter and $[h]_{\uparrow 2^i}$ as well as the $[q_{\alpha_j}]_{\uparrow 2^i}$ are FIR filters.

It is obvious that this projection can be calculated by using the cascade of digital IIR and FIR filters shown in Fig. 3. The number of octaves and sub-octaves of the scale diagram has been defined according to the desired resolution, and the smallest scale of the scale diagram has been chosen depending on the dimensions of the smallest respectively biggest expected T3DO.

When looking at the obtained scale diagram in Fig. 5 for the line scan in Fig. 4, it is obvious that possible T3DO can be recognized by the pattern "black (small coefficients) white (large coefficients) black". This information is now used for identification of the T3DO by thresholding the scale diagram twice. The final result of the identification is obtained as a mask image (Fig. 9), where the locations of the obvious T3DO of Fig. 1 can be recognized.

The question if this localized T3DO is an exposed object (grain) or a surface defect (cavity) can easily be answered, based on the images $\mathbf{U}_{\alpha_i,\beta_j}$. Because we now know the position and area of the T3DO, we can examine the grey values at this position and easily decide, if it is an exposed object or a surface defect. If the grey value curve increases in illumination direction it is a surface defect, if it decreases, it is an exposed object.

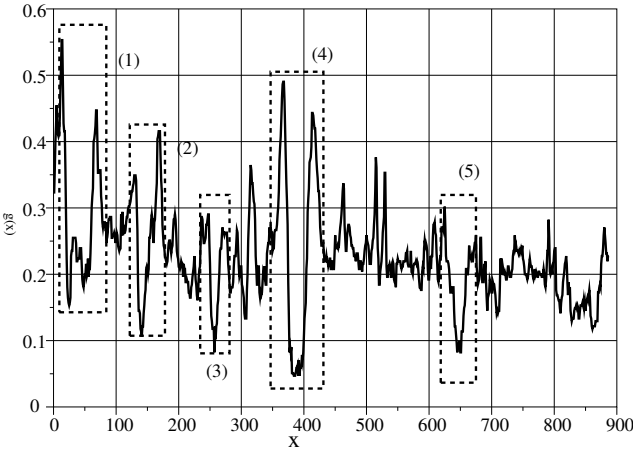

Fig. 4. Line scan of a grey value image with marked possible T3DO

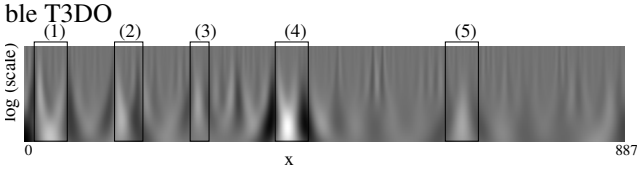

Fig. 5. Scale diagram of the signal in Fig. 4 with marked possible T3DO

4. RESULTS

The described algorithms have been applied to a high performance grinding wheel consisting of CBN grains embedded in a resin base as T3DO. Fig. 10 shows the images $\mathbf{U}_{0°,15°}$, $\mathbf{U}_{90°,15°}$, $\mathbf{U}_{180°,15°}$ and $\mathbf{U}_{270°,15°}$ (from top left to bottom right) as described in Sec. 2.

Fig. 11 shows image $\mathbf{M}_{15°}$ after combining the images $\mathbf{U}_{0°,15°}$, $\mathbf{U}_{90°,15°}$, $\mathbf{U}_{180°,15°}$, $\mathbf{U}_{270°,15°}$ according to Eq. (1). The result of the identification is presented in Fig. 12 with the corresponding histograms in Fig. 13.

5. CONCLUSIONS

The application of image processing methods, especially wavelet analysis, for monitoring the quality of grinding tools has been described. The evaluation of the 3D profile of a surface employing the consolidated image obtained by fusion of several 2-d images and subsequent wavelet analysis of line scans taken from the consolidated image yields a satisfactory inspection system. Results obtained with a CBN grinding tool are presented.

A multi–directional illumination method has been presented to acquire images with a very high degree of information from a 3-d relief by merging 2-d images. This special kind of image acquisition technique is the key for the presented method for identification of topological 3-d objects,

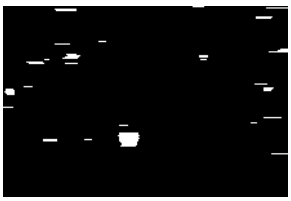

Fig. 6. Identified T3DO locations for the image rows in Fig. 1

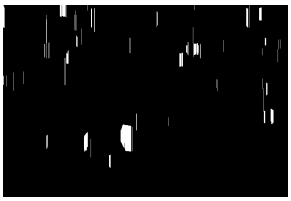

Fig. 7. Identified T3DO locations for the image columns in Fig. 1

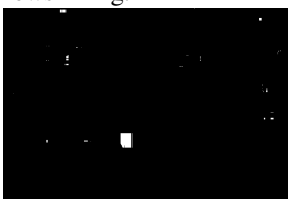

Fig. 8. Result after AND-operator applied to Fig. 6 and Fig. 7

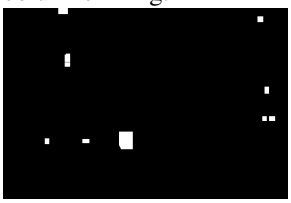

Fig. 9. Mask image: Result after morphological operations applied to Fig. 8

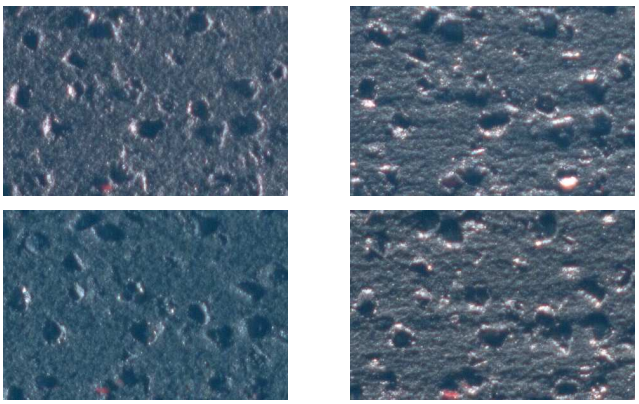

Fig. 10. Images $\mathbf{U}_{0°,15°}$, $\mathbf{U}_{90°,15°}$, $\mathbf{U}_{180°,15°}$, $\mathbf{U}_{270°,15°}$ of the same scene (grinding surface) from top left to bottom right

using the continuous wavelet transform.

The multi–directional illumination method is also the basis for further processing to get the 3D profile from the (also hybrid) reflecting and shading behavior of the single 2D images, which is straight ahead in the project. Present and future work involve the development of transformations which relate the images of surfaces obtained by multi- directional illumination with the topography.

The presented method of surface inspection of grinding tools using a suitable illumination device and wavelet analysis seems to be unique as there is no other method available

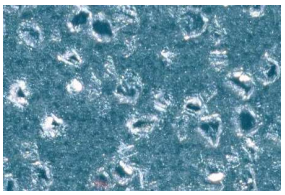

Fig. 11. $\mathbf{M}_{15°}$ taken from the images $\mathbf{U}_{0°,15°}$, $\mathbf{U}_{90°,15°}$, $\mathbf{U}_{180°,15°}$, $\mathbf{U}_{270°,15°}$

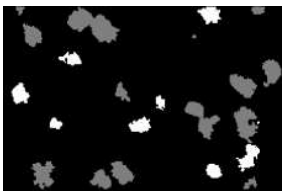

Fig. 12. Identified T3DO (grey = grain, white = cavity) of image $\mathbf{M}_{15°}$ in Fig. 11

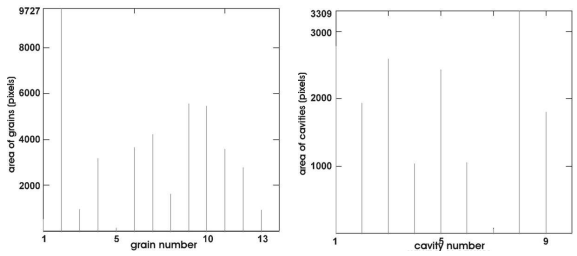

Fig. 13. Area histograms of the identified grains (left) and cavities (right) in Fig. 12

for the purpose. Performance and accuracy of the segmentation are decisive, these are best with wavelets. A visual optical differentiation between grains and cavities is practically impossible.

6. REFERENCES

[1] S. Malkin, "Grinding Technology-Theory and Application of Machining with Abrasives," *Ellis Horwood Limited*, Chichester, 1989.

[2] M. Unser, A. Aldroubi, M. Eden, "Fast b-spline Transforms for continuous Image Representation and Interpolation," *in IEEE Trans. Pattern Anal. Machine Intell., Vol.13, No. 3, pp. 277 – 285*, March 1991.

[3] M. Vrhel, C. Lee, M. Unser, "Fast Computation of the continuous Wavelet Transform through oblique Projections," *in Proc. IEEE ICASSP'96, volume III, pp. 1459–1462*, Atlanta GA, May 7-9 1996.

[4] J. Racky, M. Pandit, "Active Illumination for the Segmentation of Surface Deformations," *International Conference on Image Processing, pp. 41–45*, 1999.

[5] R. Oliver, P. Duhamel, "Fast algorithms for discrete and continuous Wavelet Transform," *in IEEE Trans. Signal Proc., Vol. 38, No. 2, pp. 569 – 585*, March 1992.